INTERNATIONAL JOURNAL OF HYDROGEN ENERGY XXX (2011) 1–10

Available at www.sciencedirect.com

journal homepage: www.elsevier.com/locate/he

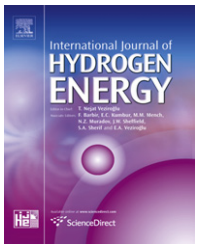

Corrosion inhibition, hydrogen evolution and antibacterial properties of newly synthesized organic inhibitors on 316L stainless steel alloy in acid medium

Nada F. Atta, A.M. Fekry, Hamdi M. Hassaneen*

Cairo University, Faculty of Science, Department of chemistry, Giza, Egypt

ARTICLE INFO

Article history:
Received 30 December 2010
Received in revised form
21 February 2011
Accepted 26 February 2011
Available online xxx

Keywords:
EIS
Hydrogen evolution
SEM
316L stainless steel
Organic inhibitors

ABSTRACT

Electrochemical corrosion behavior and hydrogen evolution reaction of 316L stainless steel has been investigated, in 0.5 M sulfuric acid solution containing four novel organic inhibitors as derivatives from one family, using potentiodynamic polarization, electrochemical impedance spectroscopy (EIS) measurements and surface examination via scanning electron microscope (SEM) technique. The effect of corrosion inhibitors on the hydrogen evolution reaction was related to the chemical composition, concentration and structure of the inhibitor. The inhibition efficiency, for active centers of the four used compounds, was found to increase in the order: $-Cl < -Br < -CH_3 < -OCH_3$. The corrosion rate and hydrogen evolution using the compound with methoxy group as a novel compound was found to increase with either increasing temperature or decreasing its concentration as observed by polarization technique and confirmed by EIS measurements. The compound with methoxy group (newly synthesized) has very good inhibition efficiency (IE) in 0.5 M sulfuric acid (98.3% for 1.0 mM concentration). EIS results were confirmed by surface examination. Also, antibacterial activity of these organic inhibitors was studied. The results showed that the highest inhibition efficiency was observed for the compound that posses the highest antibacterial activity.

Copyright © 2011, Hydrogen Energy Publications, LLC. Published by Elsevier Ltd. All rights reserved.

1. Introduction

'Stainless steel' covers a wide range of steel types and grades for corrosion or oxidation resistant applications. The main requirement for stainless steels is that they should be corrosion resistant for a specified application or environment. The selection of a particular "type" and "grade" of stainless steel must initially meet the corrosion resistance requirements [1]. Additional mechanical or physical properties may also need to be considered to achieve the overall service performance requirements. 316L stainless steel alloy (similar to 304 with Mo added to increase opposition to various forms of deterioration), offers the most resistance to corrosion in numerous standard services. The lower carbon 'variants' (316L) were established as alternatives to the 'standards' (316) carbon range grade to overcome the risk of intercystalline corrosion (weld decay), which was identified as a problem in the early days of the application of these steels [1]. Applications include cooking utensils, textiles, food processing equipments, exterior architecture, equipments for the chemical industry, truck tailors, and kitchen sinks [2]. Corrosion is a process contributing to economic losses and pollution of our environment. Thus the use of organic inhibitors is one of the most practical methods to protect metals and alloys against corrosion, especially in acid

* *Corresponding author*. Tel.: +20 202 35868682.
E-mail address: hham4@hotmail.com (A.M. Fekry).

0360-3199/$ – see front matter Copyright © 2011, Hydrogen Energy Publications, LLC. Published by Elsevier Ltd. All rights reserved.
doi:10.1016/j.ijhydene.2011.02.134

Please cite this article in press as: Atta NF, et al., Corrosion inhibition, hydrogen evolution and antibacterial properties of newly synthesized organic inhibitors on 316L stainless steel alloy in acid medium, International Journal of Hydrogen Energy (2011), doi:10.1016/j.ijhydene.2011.02.134

media [3]. The inhibition of corrosion for iron in acid solution by organic inhibitors has been studied in considerable detail [3,4]. Among alternative corrosion inhibitors, organic products containing one or more polar functions (with N, O and S atoms) have been shown to be quite efficient in preventing corrosion, in addition to heterocyclic compounds containing polar groups and π-electrons [5]. The inhibiting action of these organic compounds is usually attributed to interactions with metallic surfaces by adsorption. Considering the inhibition for corrosion of 316L stainless steel alloy, the effective inhibitors should suppress both corrosion and hydrogen evolution. The sources of hydrogen are water decomposition and reaction of water with the metal [6]. The requirement for effective inhibition of hydrogen uptake is to inhibit the hydrogen evolution, to promote the hydrogen gas recombination and to inhibit the hydrogen entry [7]. The number of adsorption active centers, the charge density, the mode of adsorption, and the projected area of the organic inhibitor could affect the inhibitor efficiency, and also the influence of the molecular area and molecular weight [8] of the organic molecule. Recently a number of studies have been focusing on the relationship between the structural properties of the organic inhibitor molecules and their inhibitory effects, in order to appraise the organic compounds as inhibitors and to design novel inhibitors for vested purpose.

This work aims to find a good corrosion inhibitor for 316L stainless steel in acid medium that makes that alloy to be used in chemical industry and to examine the resistance of the film toward the bacteria which affects the film efficiency. Thus, hydrogen evolution and corrosion behavior of 316L stainless steel was investigated in 0.5 M H_2SO_4 acid solution containing different newly synthesized organic inhibitors (A–D) [9]. Antibacterial activity of these organic inhibitors was studied. Different techniques were employed such as potentiodynamic polarization, impedance spectroscopy (EIS) and Scanning electron microscopy (SEM).

2. Experimental

2.1. Materials preparation

The tested 316L stainless steel rod has cross-sectional area of 0.2 cm^2. The composition of the stainless steel is as follows (wt %): C = 0.016, Cr = 16.71, Mo = 2.07, Ni = 10.28, N = 0.067, Mn = 1.66, Si = 0.48, P = 0.02, S = 0.00006, Cu = 0.12 and balance Fe. The test aqueous solutions contained naturally aerated solution, as present in natural environment (without agitation) H_2SO_4 (Aldrish) analytical reagents with concentration (0.5 M). Triple distilled water was used for preparing the solution. The surface of the test electrode was mechanically polished by emery papers with 400 up to 1000 grit to ensure the same surface roughness, degreasing in acetone, rinsing with ethanol and drying in air.

2.2. Electrochemical techniques

The cell used was a typical three-electrode one fitted with a large platinum sheet of size 15 × 20 × 2 mm as a counter electrode (CE), saturated calomel (SCE) as a reference electrode (RE) and 316L stainless steel alloy as the working electrode (WE). Polarization and electrochemical impedance spectroscopy (EIS) measurements were carried out using the electrochemical workstation VoltaLab/Radiometer analytical (PGZ 301). The excitation AC signal had amplitude of 10 mV peak to peak in a frequency domain from 0.1 Hz to 100 kHz. The EIS was recorded after reaching a steady state open-circuit potential. The scanning was carried out at a rate of 1 mV/s over the potential range from −500 to +200 mV vs. saturated calomel electrode (SCE). Prior to the potential sweep, the electrode was left under open-circuit in the respective solution for ~2 h until a steady free corrosion potential was recorded. Corrosion current, i_{corr}, which is equivalent to the corrosion rate is given by the intersection of the Tafel lines extrapolation. Due to the presence of a degree of nonlinearity in the Tafel slope part of the obtained polarization curves, the Tafel constants were calculated as a slope of the points after E_{corr} by ±50 mV using a computer least-squares analysis. I_{corr} were determined by the intersection of the cathodic Tafel line with the open-circuit potential. SEM micrographs were collected using a JEOL JXA-840A electron probe microanalyzer. To study the effect of temperature, the cell was immersed in water thermostat. The experiments were always carried out at 298 K, unless otherwise stated.

2.3. Organic inhibitors preparation

Synthesis of 1-aryl-3-phenylcarbamoyl-8,9-dimethoxy-10b-methyl [1,2,4]triazolo [3,4-a] 1,5,6,10b-tetrahydro-isoquinoline 4A-D. To a solution of hydrazonoyl chloride 1 (5 mmol) and 6,7-dimethoxyisoquinoline 2 (5 mmol) in tetrahydrofuran (40 ml), a triethylamine (1.4 ml (5 mmol)) was added at room temperature. The reaction mixture was refluxed for 6 h. The solvent was evaporated under reduced pressure and the residue was triturated with methanol (10 ml) where it solidified. The crude product was collected and crystallized from ethanol. The four compounds prepared with their physical constants are given below:

a-4A had mp 100 °C, 80% yield, IR (KBr) 1685 (C=O), 3275 (NH) cm^{-1}, ^1H NMR ($CDCl_3$) δ 2.2 (S, 3H), 2.5 (m, 1H), 3.1 (m, 1H), 3.4 (S, 3H), 3.4 (m, 1H), 3.8 (S, 3H), 4.0 (S, 3H), 4.9 (m, 1H), 5.8 (S, 1H), 6.5 (S, 1H), 7.1–7.6 (m, 9H), 8.6 (S, 1H) ppm, MS. $m^+/2 = 472$.

Anal. For $C_{27}H_{28}N_4O_4$: Calcd. C, 68.23; H, 5.97; N, 11.91. Found, C, 68.41; H, 5.82; N, 11.72.

b-4B had mp 105 °C, 84% yield, IR (KBr) 1680 (C=O), 3290 (NH) cm^{-1}, ^1H NMR ($CDCl_3$) δ 2.1 (S, 3H), 2.4 (S, 3H), 2.5 (m, 1H), 3.1 (m, 1H), 3.4 (m, 1H), 3.8 (S, 3H), 3.9 (S, 3H), 4.9 (m, 1H), 5.8 (S, 1H), 6.5 (S, 1H), 7.1–7.5 (m, 9H), 8.6 (S, 1H) ppm, MS. $m^+/2 = 456$.

Anal. For $C_{27}H_{28}N_4O_3$: Calcd. C, 71.01; H, 6.18; N, 12.32. Found, C, 71.21; H, 6.30; N, 12.12.

c-4C had mp 110 °C, 82% yield, IR (KBr) 1678 (C=O), 3275 (NH) cm^{-1}, ^1H NMR (DMSO) δ 2.1 (S, 3H), 2.5 (m, 1H), 3.0 (m, 1H), 3.4 (S, 1H), 3.4 (m, 1H), 3.8 (S, 3H), 3.9 (S, 3H), 4.9 (m, 1H), 5.8 (S, 1H), 6.4 (S, 1H), 7.1–7.8 (m, 9H), 8.6 (S, 1H) ppm, MS. $m^+/2 = 520$, 522.

Anal. For $C_{26}H_{25}BrN_4O_3$: Calcd. C, 59.83; H, 4.83; N, 10.79, Br, 15.34. Found, C, 59.71; H, 4.60; N, 10.50; Br, 15.10.

d- 4D had mp 146 °C, 85% yield, IR (KBr) 1680 (C=O), 3280 (NH) cm^{-1}, ^1H NMR ($CDCl_3$) δ 2.1 (S, 3H), 2.6 (m, 1H), 3.0 (m, 1H),

Please cite this article in press as: Atta NF, et al., Corrosion inhibition, hydrogen evolution and antibacterial properties of newly synthesized organic inhibitors on 316L stainless steel alloy in acid medium, International Journal of Hydrogen Energy (2011), doi:10.1016/j.ijhydene.2011.02.134

3.3 (S, 3H), 3.4 (m, 1H), 3.8 (S, 3H), 4.9 (m, 1H), 5.8 (S, 1H), 6.5 (S, 1H), 7.1–7.9 (m, 9H), 8.6 (S, 1H) ppm, MS. $m^+/2 = 477,479$.

Anal. For $C_{26}H_{25}ClN_4O_3$: Calcd. C, 65.54; H, 5.29; N, 11.80, Cl, 7.45. Found, C, 65.33; H, 5.10; N, 11.62; Cl, 7.31.

2.4. *Antibacterial activity*

The tested compounds A–D of similar concentration (1.0 mM in 0.5 M H_2SO_4 solution) were prepared. Bacterial cell suspension was prepared by transferring of one loopful of fresh bacterial cells [10] (*Escherichia coli*) into an appropriate amount of sterilized water forming a bacterial cell suspension that was directly used for the antibacterial tests for the tested compounds [11].

Fresh liquid LB (Luria Bertani) broth medium (1% trypton, 1% NaCl and 0.5% yeast extract) (Sigma) was prepared and sterilized by autoclave at 121 °C at 15 p.s.i for 15 min. Then 10 ml of sterile LB liquid medium was transferred into sterile falcon tube (50 ml). 50 μl of each tested compound was transferred into the liquid medium and shaked at 200 RPM for 4 h at 37 °C. Antibacterial activities of the tested compounds were determined in presence of control which contains LB supplemented by 50 μl solvent (0.5 M H_2SO_4) only.

Antibacterial activity and bacterial growth inhibition was determined by measuring the optical density (OD) at 600 nm for the bacterial cultures in presence of the tested compounds relative to the control by using spectrophotometer (Jenway).

3. Results and discussion

The method for synthesis of triazoquinoline derivatives that are used as inhibitors (compounds A–D) in this work is reported in Scheme 1.The four inhibitors called compounds A–D, where A containing $-OCH_3$ group as substituent, B contains $-CH_3$ group, C contains –Br and D contains –Cl as substituents. To the best of our knowledge, the triazoloisoquinoline 4 required for this study have not yet been reported and prepared via cycloaddition of nitrilimine 2 (prepared in situ from hydrazonoyl chloride 1 and triethylamine) with 1-methylisoquinoline 3.

3.1. *EIS measurements*

The EIS scans of 316L stainless steel alloy in dependence on the type and concentration of A–D organic inhibitors were recorded after the working electrode was left in the test solution for 2 h to achieve its steady free corrosion potential (E_{st}) value with and without inhibitors. The experimental EIS are presented as Bode plots in Fig. 1a (impedance diagram), Fig. 1b (phase

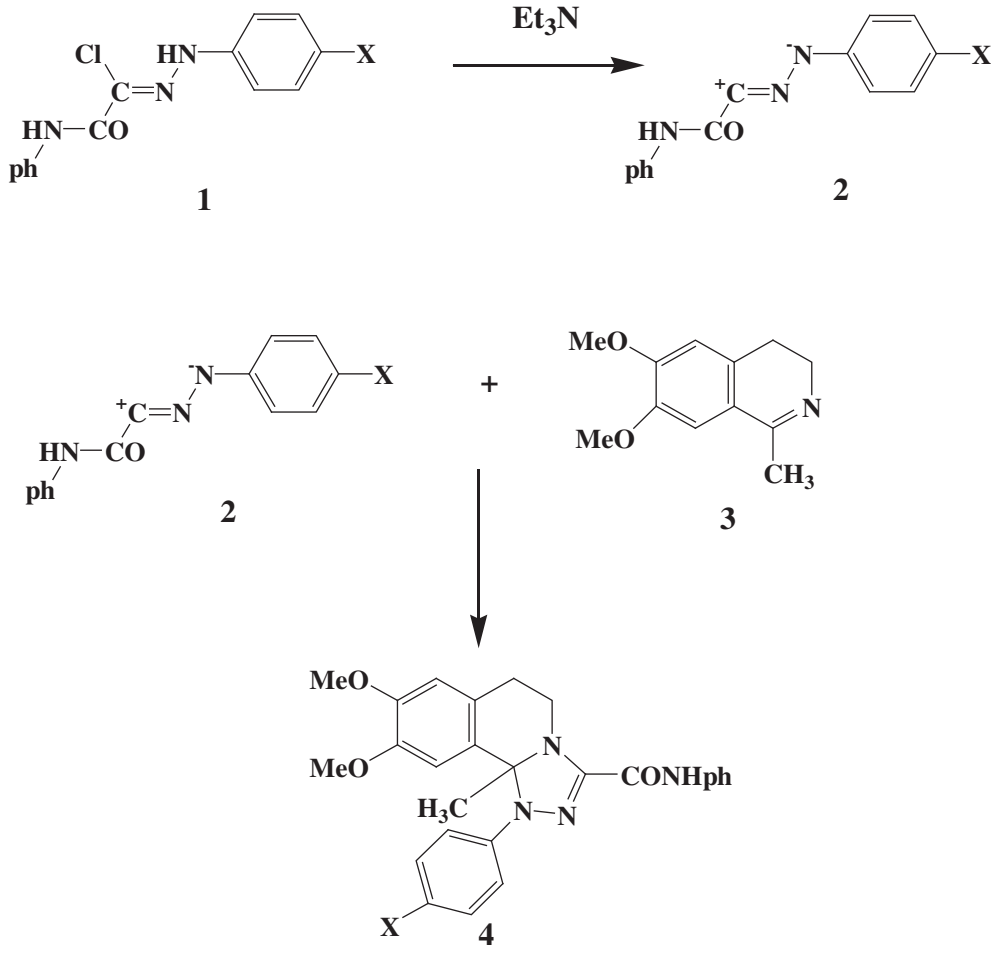

Scheme 1 – Synthesis of triazoloisoquinoline derivatives.

Please cite this article in press as: Atta NF, et al., Corrosion inhibition, hydrogen evolution and antibacterial properties of newly synthesized organic inhibitors on 316L stainless steel alloy in acid medium, International Journal of Hydrogen Energy (2011), doi:10.1016/j.ijhydene.2011.02.134

diagram) and (Nyquist plots) in Fig. 1c, for compounds A–D. The impedance (|Z|) of 316L stainless steel alloy is clearly found to depend on the inhibitor type. The impedance data were thus simulated to the appropriate equivalent circuit (Fig. 2). This simulation gave a reasonable fit with an average error of about 3%. The estimated data is given in Table 1. The appropriate equivalent model used to fit the high and low frequency data consists of R_s (solution resistance), C is related to the contribution from the capacitance of the surface film, R is the respective resistance of the surface film and Z_W is a Warburg impedance due to ion diffusion [12] through the passive film. Such diffusion process may indicate that the corrosion mechanism is controlled not only by a charge-transfer process but also by a diffusion process [13]. Analysis of the experimental spectra were made by best fitting to the corresponding equivalent circuit using Zview software provided with the VoltaLab workstation where the dispersion formula suitable to each model was used. In all cases, good conformity between theoretical and experimental was obtained for the whole frequency range with an average error of 3%.

Regarding the influence of active centers of the four organic inhibitors on the film resistance of 316L stainless steel alloy surface film, which is inversely proportional to the capacitance (C) of the film [13]. As shown in Table 1, R value of the four inhibitors is higher than that of the blank (0.5 M H_2SO_4) and is in the following order A > B > C > D > blank, which is due to the difference in the substituents (the active centers) in each compound: $-OCH_3$ > $-CH_3$ > $-Br$ > $-Cl$, respectively. Compound A has the highest film resistance value because it has the most electron rich environment due to its more donating property of methoxy group compared to compound B which contains methyl group. Such action could be explained through the lone pair of non-bonding electrons on $-OCH_3$ group which are freely to liberate its lone pair into the system than methyl group. Also, $-Cl$ anion is more electron withdrawing than $-Br$, due to its higher electronegativity which leads to lower inhibition efficiency. It is known that the rate of adsorption is usually rapid and hence, the reactive metal surface is shielded from the aggressive acid environment and thus decreasing hydrogen evolution on the electrode surface [5].

Compound A shows the highest film resistance. On studying the effect of different concentrations (Fig. 3) on the film resistance R and the relative thickness (1/C), the results show that they increase by increasing inhibitor concentration in 0.5 M H_2SO_4, however the hydrogen evolution rate decreases. The data of impedance parameters of 316L stainless steel alloy in different concentration of compound A in 0.5 M sulfuric acid at 298 K (Table 2) illustrates that an increase in inhibitor concentration leads to an increase in the R, W and decrease in C values or rate of hydrogen evolution. Since the

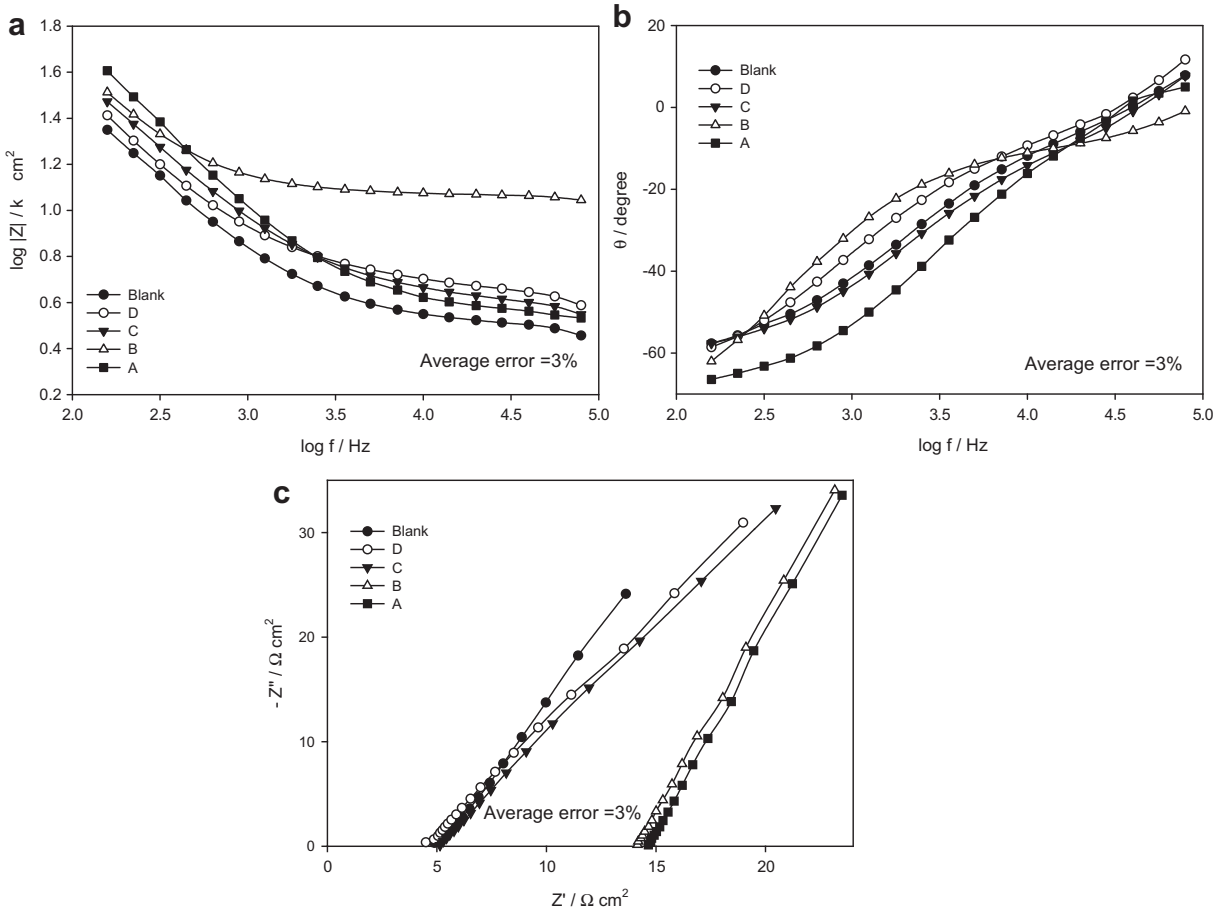

Fig. 1 – Bode plots as (a) impedance; (b) phase diagrams and (c) Nyquist plots for 316L stainless steel alloy in 0.5 M H_2SO_4 acid containing different inhibitors of 1.0 mM concentration at 298 K.

Please cite this article in press as: Atta NF, et al., Corrosion inhibition, hydrogen evolution and antibacterial properties of newly synthesized organic inhibitors on 316L stainless steel alloy in acid medium, International Journal of Hydrogen Energy (2011), doi:10.1016/j.ijhydene.2011.02.134

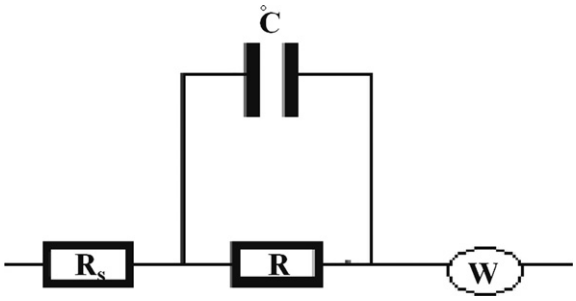

Fig. 2 – Equivalent circuit model representing one time constant for an electrode/electrolyte solution interface.

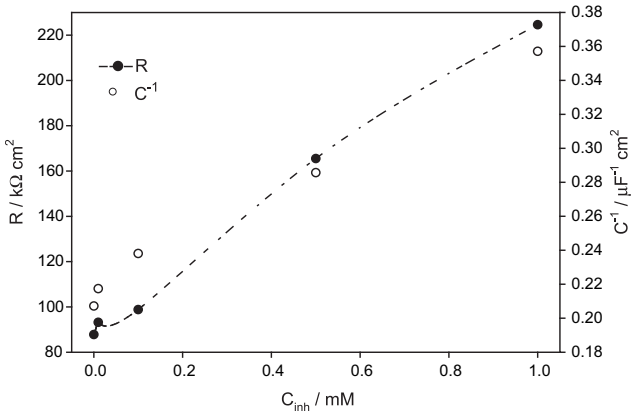

Fig. 3 – Variation of film resistance (R) or relative thickness (C^{-1}) with concentration for compound A in 0.5 M H_2SO_4 solution, at 298 K.

passive oxide film can be considered as a dielectric plate capacitor, the passive film thickness (d) in cm is related to the capacitance (C) by the equation [14]:

$$d = \epsilon_o \epsilon_r A/C \quad (1)$$

where ϵ_o is the vacuum permittivity (8.85×10^{-12} Fcm^{-1}), ϵ_r is the relative dielectric constant of the film and A is the electrode area in cm^2. Although the actual value of ϵ_r within the film is difficult to estimate, a change of C can be used as an indicator for change in the film thickness. Hence, the reciprocal capacitance (1/C) of the surface film is directly proportional to its thickness. Thus, when inhibitor concentration increases, more inhibitor molecules will be adsorbed on the surface through the active centers in compound A, double bonds or heteroatoms (oxygen or nitrogen) which leads to increase in film thickness and decrease in hydrogen evolution.

The total resistance (R) for compound A is the highest and for compound D is the lowest at 1.0 mM concentration of the inhibitor in acid medium as confirmed by SEM micrographs (Fig. 4d, b), respectively, compared to the blank (0.5 M H_2SO_4) in Fig. 4a. Compound A shows a denser and smoother film adsorbed on the alloy surface than that of compound D, which is more smoother than that of the blank Fig. 4b. Also, on comparing 1.0 mM concentration for Compound A (Fig. 4d) and 0.01 mM of the same compound (Fig. 4c), it has been observed that the film is thicker for higher concentration of Compound A (1.0 mM concentration in 0.5 M sulfuric acid solution).

On studying compound A of 1.0 mM concentration in 0.5 M sulfuric acid solution at different temperatures as shown in Fig. 5a,b as Bode plots (impedance and phase diagrams), it has been found that impedance value decrease with increasing temperature. The plots are best fitted to the same model shown in Fig. 2 and the estimated parameters are given in Table 3 for inhibited tested alloy. Higher temperatures can decrease film growth process due to enhanced solubility of the corrosion products and increasing hydrogen evolution, leading to a significant decrease in surface film stability. Also, Warburg impedance values decrease with increasing temperature for inhibited alloy.

3.2. *Potentiodynamic polarization measurements*

Potentiodynamic polarization behavior of 316L stainless steel was studied in relation to inhibitor type and concentration. The potential was scanned automatically from −0.5 to 0.2 V vs. SCE at a rate of 1 mV s^{-1} which allows the quasi-stationary state measurements. Prior to the potential scan the electrode was left under open-circuit conditions in the respective solution for 2 h until a steady free corrosion potential (E_{st}) value was recorded. Fig. 6 shows linear sweep potentiodynamic traces for the steel in 0.5 M H_2SO_4 containing different substituted derivatives of organic inhibitor. As was observed from impedance results, compound A has the lowest corrosion current density and lowest corrosion rate as given in Table 4. This is due to the active center methoxy group. Thus it has the highest inhibition efficiency as shown in Table 4. The inhibition efficiency (IE %) is calculated from the following equation [5]:

Table 1 – Impedance parameters of 316L stainless steel alloy in 0.5 M H_2SO_4 acid containing different inhibitors of 1.0 mM concentration at 298 K.

Compound	R_s (Ω cm^2)	R ($k\Omega$ cm^2)	C (μF cm^{-2})	W Ω cm^2 $s^{-1/2}$
Blank	4.9	87.8	4.83	3.57
A	13.9	224.6	2.80	4.45
B	14.4	215.9	2.84	4.13
C	4.8	110.5	2.89	4.08
D	4.6	104.3	2.89	3.83

Table 2 – Impedance parameters of 316L stainless steel alloy in 0.5 M H_2SO_4 acid containing compound A with different concentrations at 298 K.

Conc. mM	R_s (Ω cm^2)	R ($k\Omega$ cm^2)	C (μF cm^{-2})	W Ω cm^2 $s^{-1/2}$
0	4.9	87.8	4.83	3.57
1	13.9	224.6	2.80	5.01
0.5	4.3	165.5	3.50	4.45
0.1	6.7	98.8	4.20	3.78
0.01	5.5	93.2	4.60	3.75

Please cite this article in press as: Atta NF, et al., Corrosion inhibition, hydrogen evolution and antibacterial properties of newly synthesized organic inhibitors on 316L stainless steel alloy in acid medium, International Journal of Hydrogen Energy (2011), doi:10.1016/j.ijhydene.2011.02.134

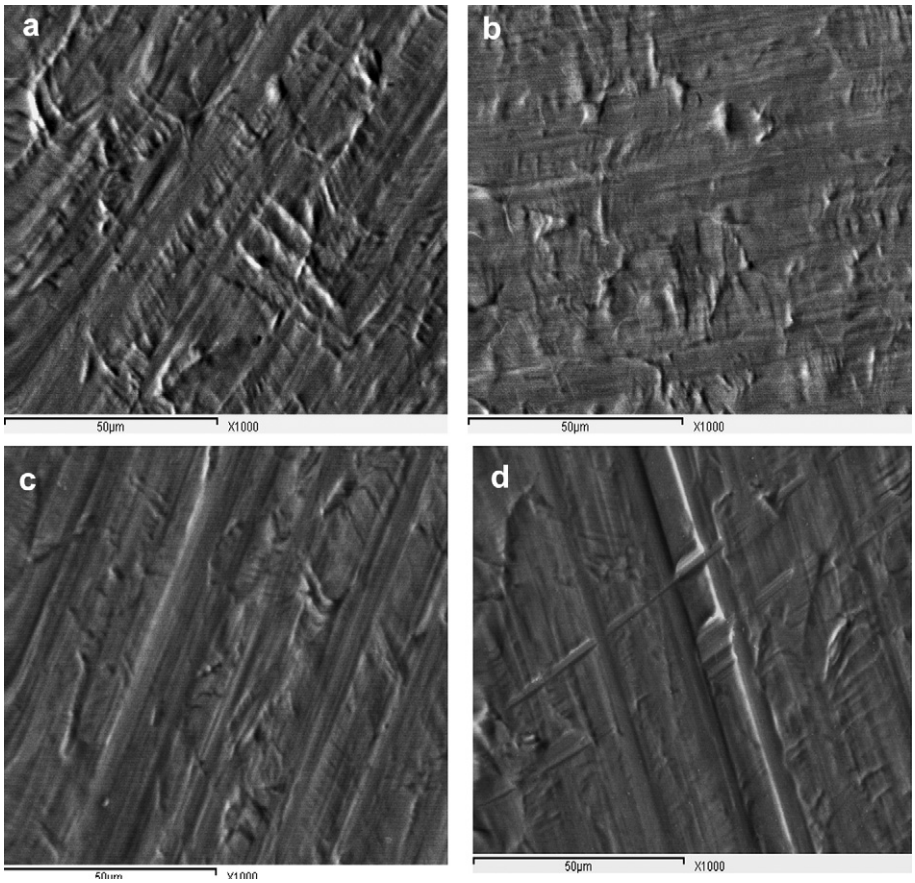

Fig. 4 – SEM micrographs of 316L stainless steel alloy after immersion for 2 h in (a) blank (0.5 M H_2SO_4 solution), (b) Compound D (1.0 mM/Cl^-) (c) compound A (0.01 mM/CH_3O) and (d) compound A (1.0 mM/CH_3O) in 0.5 M sulfuric acid containing solution, at 298 K.

$$IE\% = 1 - \frac{i_{inh}}{i_{corr}} \times 100 \quad (2)$$

where i_{corr} and i_{inh} are the uninhibited and inhibited corrosion current densities, respectively.

On studying the effect of concentration for this compound from 10^{-3} to 10^{-5} mM, it is noticed that the corrosion potential shifts slightly toward more positive potential (Fig. 7) as the inhibitor concentration increases. This is characteristic of spontaneous passivation as a result of the development of an oxide film. The behavior indicates that the cathodic processes predominant over the anodic ones. The necessary electrons of the cathodic reaction are provided by the ionization of metal atoms (most probably Cr atoms) entering the oxide phase. Also, corrosion current density value decreases with increasing inhibitor concentration as given in Table 5. This indicates that this inhibitor promotes passivation of 316L stainless steel through adsorption and decreasing hydrogen evolution. This also can be attributed to deposition of the inhibitor molecules by increasing concentration on the alloy as a result of interaction between the inhibitor and the metal surface especially Cr, Ni and Mo that can form oxides which effectively seals the surface against further reaction. Hydrogen evolution reaction has been reported [15] to be generally the dominant local cathodic process in the corrosion of 316L stainless steel alloy in aqueous acidic solutions, via H^+ ion or H_2O molecule reduction, respectively. The amounts of hydrogen evolved by the cathodic reaction are proportional to the corroded amounts of iron [8]. The increase of the corrosion rate and rate of hydrogen evolution can be rationalized on the basis that sulfuric acid reacts with iron and forms metal sulphates, which are soluble in aqueous media [7]. There are two reactions occur the anodic reaction and cathodic reaction. The following equations represent iron reaction in acidic solutions [16]:

Anodic reaction (Oxidation reaction)

$$Fe \rightarrow Fe^{2+} + 2e \quad (3)$$

Cathodic (Reduction reaction or hydrogen evolution reaction)

$$2H^+ + 2e \rightarrow H_2\uparrow \quad (4)$$

The increase of inhibitor concentration leads to an increase in inhibition efficiency which may be due to the blocking effect of the surface by both adsorption and film formation mechanism which decreases the effective area of attack. The change of cathodic and anodic Tafel slopes alters

Please cite this article in press as: Atta NF, et al., Corrosion inhibition, hydrogen evolution and antibacterial properties of newly synthesized organic inhibitors on 316L stainless steel alloy in acid medium, International Journal of Hydrogen Energy (2011), doi:10.1016/j.ijhydene.2011.02.134

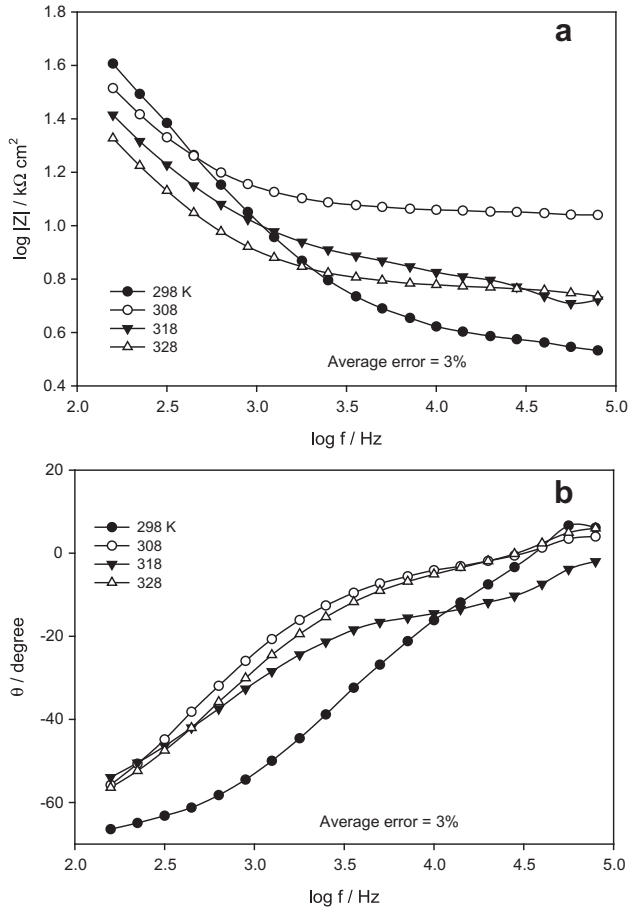

Fig. 5 – Bode plots as (a) impedance and (b) phase diagrams for 316L stainless steel alloy in 0.5 M H_2SO_4 acid containing compound A of 1.0 mM concentration at different temperatures.

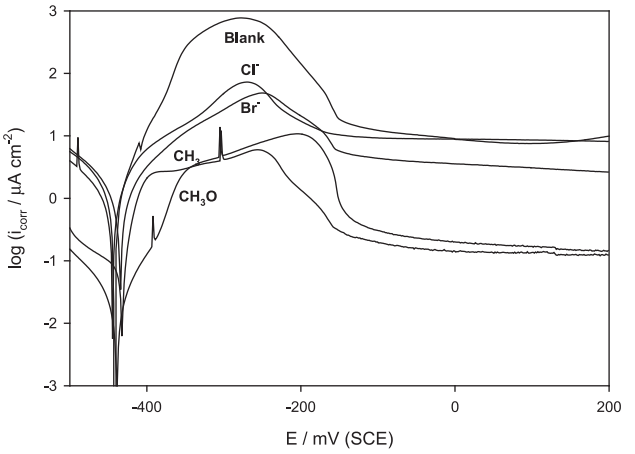

Fig. 6 – Potentiodynamic polarization scans of 316L stainless steel alloy in 0.5 M H_2SO_4 acid containing different inhibitors of 1.0 mM concentration at 298 K.

unremarkably (Fig. 7). This is indicative that compound A acts as mixed inhibitors by merely blocking the reaction sites of the metal surface without changing the anodic and cathodic reaction mechanisms [5,7]. Results of the inhibition efficiencies revealed the good inhibiting action of compound A reaching to 98.3% at 1.0 mM concentration at 298 K. The highest IE exhibited by the compound may be attributed to its adsorption on the metal surface through polar groups (–OCH_3, N or O) as well as through π-electrons of the double bond. Hydrogen evolution is also important for hydrogenation reactions in acid medium as sulfuric acid. The HER is one of the simplest and most fundamentally important reactions in electrochemistry. It has received great attention from corrosion engineers and scientists because of its crucial role in the corrosion of many metals in acid media. The reaction is also of basic importance in the related problem of hydrogen embrittlement, since it controls the hydrogen entrance into metals from aqueous solution. Following mechanisms can be proposed for HER on electrodes in acidic media [17]:

1. a primary discharge step (Volmer reaction)

$$M + H_3O^+ + e \leftrightarrow MH_{ad} + H_2O \quad (5)$$

2. an electrochemical-desorption step (Heyrowsky reaction)

$$MH_{ad} + H_3O^+ + e \rightarrow M + H_2 + H_2O \quad (6)$$

3. a recombination step (Tafel reaction)

$$MH_{ad} + MH_{ad} \rightarrow 2M + H_2 \quad (7)$$

For hydrogen evolution reaction, the cathodic reaction may have three different steps: first, water molecule or hydronium ion is discharged on electrode surface to produce hydrogen atom in acidic solution then three states for the formulation of the mechanism occurs [18], no one of the three reactions formulated occurs as a single step but combines with another; i.e. Volmer reaction (slow) with the following Heyrowsky (faster) or Tafel (faster) reaction must be. If Volmer reaction is fast, Tafel and/or Heyrowsky reaction must be slow. The step of a slow reaction follows by a fast step. So, presence of inhibitors may hinder the formation of MH_{ad} and supress reaction (5) or hinder the electron transfer to H_3O^+ ion and suppress reaction (6).

In a corrosive environment, the majority of the adsorbed atomic hydrogen (MH_{ads}) will recombine and form molecular hydrogen, which accumulates and bubbles off of the surface. This recombination of the adsorbed hydrogen atoms is the

Table 3 – Impedance parameters of 316L stainless steel alloy in 0.5 M H_2SO_4 acid containing 1.0 mM of compound A at different temperatures.

T (K)	R_s (Ω cm²)	R (kΩ cm²)	C (μF cm^{-2})	W Ω cm² s$^{-1/2}$
298	13.9	224.6	2.8	5.01
308	3.34	130.8	2.9	3.26
318	5.69	73.78	3.9	2.11
328	5.66	70.91	4.5	1.83

Please cite this article in press as: Atta NF, et al., Corrosion inhibition, hydrogen evolution and antibacterial properties of newly synthesized organic inhibitors on 316L stainless steel alloy in acid medium, International Journal of Hydrogen Energy (2011), doi:10.1016/j.ijhydene.2011.02.134

Table 4 – Polarization parameters of 316L stainless steel alloy in 0.5 M H_2SO_4 acid containing different inhibitors of 1.0 mM concentration at 298 K.

Compound	$-\beta_c$ (mV/decade)	β_a (mV/decade)	i_{corr} (μA cm^{-2})	E_{corr} (mV)	IE%
Blank	127.0	132.0	2.09	−445.0	0.0
A	135.5	111.6	0.04	−440.0	98.1
B	132.0	47.4	0.27	−437.0	87.1
C	125.0	88.0	0.83	−435.0	60.3
D	145.0	145.3	1.01	−444.5	51.7

second step of the HER. This step can take place through an atom–atom combination as suggested by the chemical recombination mechanism (Tafel–Volmer) or through an ion–atom reaction as suggested by the electrochemical recombination mechanism (Volmer–Heyrovsky).

On studying the effect of temperature for compound A of 1.0 mM concentration to evaluate the activation parameters of the corrosion processes of 316L stainless steel in acidic media, polarization parameters are investigated for compound A at temperature range of 298–328 K and presented in Table 6. Fig. 8 shows the polarization curve of 1.0 mM inhibited tested alloy. The values of i_{corr} increase with temperature indicating activation in the dissolution process of the surface oxide film associated with a reduction in its protective properties. This may be attributed to some intrinsic modifications made by the film in its chemical composition and/or physical structure [14]. The corrosiveness is significantly limited in the presence of inhibitor and it can be seen that the corrosion current density for tested sample increases to a slow extend with temperature. This confirms that compound A acts as an efficient corrosion inhibitor with maximum inhibition efficiency at 298 K (98.3%).

The apparent activation energy, E_a, of the corrosion reaction was determined using Arrhenius plots. Arrhenius equation could be written as:

$$i_{corr} = Ae^{-Ea/RT} \quad (8)$$

where i_{corr} is the corrosion current density, E_a the apparent activation factor. The apparent activation energy of the corrosion reaction could be determined by plotting log i_{corr} against 1/T which gives a straight line with a slope permitting the determination of E_a as shown in Fig. 8. The calculated value of the apparent activation corrosion energy is 8.02 kJ mol^{-1} assigning a diffusion controlled reaction. The high activation energy value indicates the high inhibition efficiency of the inhibitor.

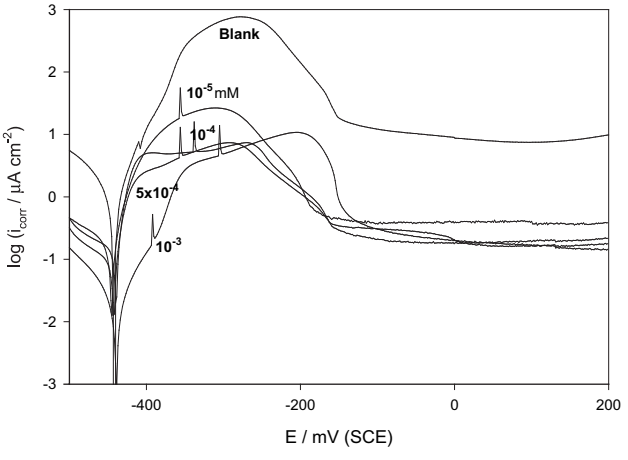

Fig. 7 – Potentiodynamic polarization scans of 316L stainless steel alloy in 0.5 M H_2SO_4 acid containing compound A of different concentrations, at 298 K.

3.3. *Adsorption isotherm*

Data obtained from polarization measurements were tested graphically for fitting various isotherms including Langmuir, Frumkin and Temkin. Compound A gives the best fit with Langmuir isotherm (Fig. 8). According to this isotherm θ is related to inhibitor concentration.

$$\frac{C}{\theta} = \frac{1}{K_{ads}} + C \quad (9)$$

K_{ads} is the adsorption–desorption equilibrium constant. From the intercept, K_{ads} value was calculated for the adsorption process to be 0.02×10^4 M^{-1}. However, the slope (1.03) of the relation shows a little deviation from unity, this might be the result from the interactions between the adsorbed species on the metal surface [5]. The K_{ads} value may be taken as a measure of the strength for the adsorption forces between the inhibitor molecules and the metal surface. The adsorption equilibrium constant, K_{ads}, is related to the standard free energy, ΔG°_{ads}, with the following equation:

$$K_{ads} = \frac{1}{55.5}\exp\frac{-\Delta G^\circ_{ads}}{R\,T} \quad (10)$$

The relation between log K_{ads} and T^{-1} deduced ΔG°_{ads} which is equal to −9.8 kJ mol^{-1}.

The negative values of ΔG°_{ads} ensure the spontaneity of the adsorption process and the stability of the adsorbed layer on the steel surface. It is well known that values of ΔG°_{ads} in the order of −20 kJ mol^{-1} or lower indicate a physisorption; those of order of −40 kJ mol^{-1} or higher involve charge sharing or transfer from the inhibitor molecules to the metal surface to form a coordinate type of bond (chemisorption) [5]. The calculated ΔG°_{ads} value indicates that the adsorption mechanism of compound A on mild steel in 0.5 M H_2SO_4 solution is typical of physisorption. The inhibition behavior is attributed to the electrostatic interaction between the organic molecules and iron atom [19].

By using the transition state equation:

$$\log\left(\frac{i_{corr}}{T}\right) = \log\frac{R}{Nh} + \frac{\Delta S^o_{ads}}{2.303R} - \frac{\Delta H^o_{ads}}{2.303RT} \quad (11)$$

where N is the Avogadro's number and h is the Plank constant. Hence, a plot of log i_{corr}/T against 1/T yields a straight line as

Please cite this article in press as: Atta NF, et al., Corrosion inhibition, hydrogen evolution and antibacterial properties of newly synthesized organic inhibitors on 316L stainless steel alloy in acid medium, International Journal of Hydrogen Energy (2011), doi:10.1016/j.ijhydene.2011.02.134

Table 5 – Polarization parameters of 316L stainless steel alloy in 0.5 M H_2SO_4 acid containing compound A with different concentrations at 298 K.

Conc. mM	$-\beta_c$ (mV/decade)	β_a (mV/decade)	i_{corr} ($\mu A\ cm^{-2}$)	E_{corr} (mV)	IE%
0	127.0	132.0	2.09	−445.0	0.0
1	135.5	111.6	0.04	−440.0	98.1
0.5	106.0	180.1	0.11	−441.6	94.7
0.1	89.1	198.0	0.16	−449.4	92.3
0.01	85.4	241.0	0.21	−449.6	90.0

shown in Fig. 9 and the standard enthalpy change ΔH°_{ads} can be evaluated from the slope and found to be −12.56 kJ mol^{-1}. The standard adsorption entropy ΔS°_{ads} are calculated to be 75.02 J mol^{-1} K^{-1} according to the following thermodynamic basic equation:

$$\Delta G^{o}_{ads} = \Delta H^{o}_{ads} - T\Delta S^{o}_{ads} \quad (12)$$

The ΔS°_{ads} value is large and positive (94.9 J mol^{-1} K^{-1}), meaning that an increase in disordering takes place in going from reactants to the metal-adsorbed species reaction complex.

3.4. *Antibacterial activity*

Antibacterial activity test illustrates that the inhibitors A–D have different antibacterial activities on tested micro-organisms. The test was done by measuring the optical density [20] of the bacterial growth in presence of each compound relative to the control (LB + solvent) Table 7. The lowest measured OD was found for compound A and the highest OD was for compound D.

Therefore according to the obtained results, the order of antibacterial activity of the tested inhibitors is as follows: A > B > C > D, which means that compound D is of lowest antibacterial activity and compound A is of highest antibacterial activity. This means that compound D affected by bacteria more than other compounds and thus its corrosion or hydrogen evolution rate is the highest, however, compound A doesn't affected well by bacteria, so, its corrosion or hydrogen evolution rate is the lowest relative to other used inhibitors.

So, from the previous results, the highest inhibition efficiency obtained and the highest antibacterial activity were found for compound A [20–22]. This shows that the antibacterial activity results are in good agreement with the experimental data of polarization, impedance or SEM results. Thus,

Table 6 – Polarization parameters of 316L stainless steel alloy in 0.5 M H_2SO_4 acid with and without 1.0 mM of compound A at different temperatures.

T (K)	$-\beta_c$ (mV/decade)	β_a (mV/decade)	i_{corr} ($\mu A\ cm^{-2}$)	E_{corr} mV	IE%
298	127.0	132.0	2.09	−445.0	
308	129.1	143.5	2.21	−449.7	
318	132.2	140.7	2.42	−455.3	
328	126.3	138.5	2.50	−453.5	
298	135.5	111.6	0.04	−440.0	98.1
308	130.3	124.8	0.05	−438.0	97.7
318	112.5	125.5	0.06	−448.1	97.5
328	132.4	130.9	0.07	−449.4	97.2

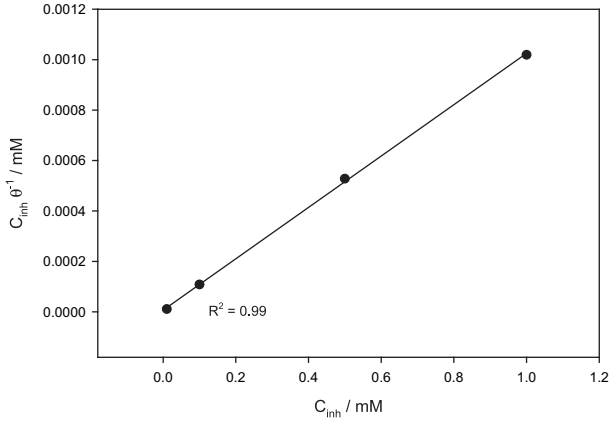

Fig. 8 – Langmuir isotherm adsorption model on mild steel surface of Compound A in 0.5 M H_2SO_4 solution, at 298 K.

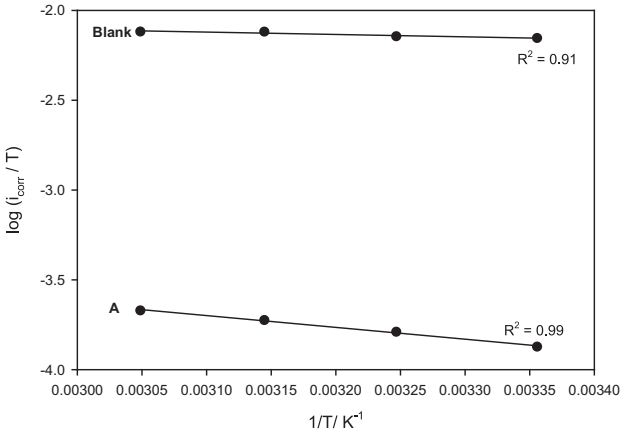

Fig. 9 – Variation of log i_{corr}/T with 1/T for 316L stainless steel alloy in 0.5 M H_2SO_4 acid containing compound A of 1.0 mM concentration at different temperatures.

Table 7 – The optical density (OD_{600}) of the bacterial growth in presence of each compound relative to the control.

Compounds	OD_{600}
Control (LB + solvent)	0.900
Compound A/CH_3O	0.067
Compound B/CH_3	0.082
Compound C/Br^-	0.123
Compound D/Cl^-	0.449

Please cite this article in press as: Atta NF, et al., Corrosion inhibition, hydrogen evolution and antibacterial properties of newly synthesized organic inhibitors on 316L stainless steel alloy in acid medium, International Journal of Hydrogen Energy (2011), doi:10.1016/j.ijhydene.2011.02.134

compound A, that shows a denser and smoother surface adsorbed film, has highest antibacterial activity that is the surface film formed doesn't deteriorate or affected by bacteria due to its high antibacterial activity. This leads to a film of high corrosion resistance, low corrosion current density and high efficiency.

4. Conclusions

- EIS results showed that using 0.5 M sulfuric acid medium containing compound A as inhibitor for 316L alloy gives the highest corrosion resistance (R_T) value relative to the other used compounds (B, C and D).
- Polarization results showed that corrosion current density (i_{corr}) value or hydrogen evolution rate is the lowest for compound A and these results confirmed well EIS results.
- The corrosion (i_{corr}) and hydrogen evolution rate, for compound A, were found to increase with either increasing temperature or decreasing inhibitor concentration.
- All obtained results are confirmed by measuring antibacterial activity, where compound A shows the highest antibacterial activity due to the high resistance of the organic film inhibitor formed which doesn't affect or deteriorate by the action of the bacteria.
- Generally, EIS measurements were confirmed by polarization results, antibacterial activity and scanning electron micrographs.

REFERENCES

[1] De Renzo DJ, Mellan I. Corrosion resistant materials handbook. 4th ed.; 1985.
[2] Michler T, Lee Y, Gangloff RP, Naumann J. Influence of macro segregation on hydrogen environment embrittlement of SUS 316L stainless steel. International Journal of Hydrogen Energy 2009;34:3201.
[3] Fekry AM, Mohamed RR. Acetyl thiourea chitosan as an eco-friendly inhibitor for mild steel in sulfuric acid medium. Electrochimica Acta 2010;55:1933.
[4] Heakal FE, Fekry AM. Experimental and theoretical study of uracil and adenine inhibitors in Sn-Ag alloy/nitric acid corroding system. Journal of Electrochemical Society 2008; 155:C534.
[5] Fekry AM, Ameer MA. Corrosion inhibition of mild steel in acidic media using newly synthesized heterocyclic organic molecules. International Journal of Hydrogen Energy 2010; 34:7641.
[6] Lunarska E, Chernyayeva O. Effect of corrosion inhibitors on hydrogen uptake by Al from NaOH solution. International Journal of Hydrogen Energy 2006;31:285.
[7] Ameer MA, Fekry AM. Inhibition effect of newly synthesized heterocyclic organic molecules on corrosion of steel in alkaline medium containing chloride. International Journal of Hydrogen Energy 2010;35:11387.
[8] Muñoz LD, Bergel A, Féron D, Basséguy R. Hydrogen production by electrolysis of a phosphate solution on a stainless steel cathode. International Journal of Hydrogen Energy 2010;35:8561.
[9] Elwan NM, Abdelhadi HA, Abdallah TA, Hassaneen HM. Synthesis of [1,2,4]triazolo[3,4-a]isoquinolines and pyrrolo [2,1-a]isoquinolines using α-keto hydrazonoyl halides. Tetrahedron 1996;52:3451.
[10] Jigar MJ, Sinha VK. Ceric ammonium nitrate induced grafting of polyacrylamide onto carboxymethyl chitosan. Carbohydrate Polymers 2007;67:427.
[11] Peng X, Zhang L. Self-assembled micelles of N-phthaloyl-carboxymethychitosan for drug delivery. Colloids and Surfaces A: Physicochemical and Engineering Aspects 2009;337:21.
[12] Fekry AM. Impedance and hydrogen evolution studies on magnesium alloy in oxalic acid solution containing different anions. International Journal of Hydrogen Energy 2010;35:12945.
[13] Fekry AM, Fatayerji MZ. Electrochemical corrosion behavior of AZ91D alloy in ethylene glycol. Electrochimica Acta 2009; 54:6522.
[14] Fekry AM. The influence of chloride and sulphate ions on the corrosion behavior of Ti and Ti-6Al-4V alloy in oxalic acid. Electrochimica Acta 2009;54:3480.
[15] Heakal FE, Fekry AM, Fatayerji MZ. Influence of halides on the dissolution and passivation behavior of AZ91D magnesium alloy in aqueous solutions. Electrochimica Acta 2009;54:1545.
[16] El-Meligi AA, Ismail N. Hydrogen evolution reaction of low carbon steel electrode in hydrochloric acid as a source for hydrogen production. International Journal of Hydrogen Energy 2009;34:91.
[17] Bhardwaj M, Balasubramaniam R. Uncoupled non-linear equations method for determining kinetic parameters in case of hydrogen evolution reaction following Volmer–Heyrovsky–Tafel mechanism and Volmer–Heyrovsky mechanism. International Journal of Hydrogen Energy 2008;33:2178.
[18] Azizi O, Jafarian M, Gobal F, Heli H, Mahjani MG. The investigation of the kinetics and mechanism of hydrogen evolution reaction on tin. International Journal of Hydrogen Energy 2007;32:1755.
[19] Labjara N, Lebrinib M, Bentissc F, Chihibd NE, El Hajjaji S, Jama C. Corrosion inhibition of carbon steel and antibacterial properties of aminotris-(methylenephosphonic) acid. Materials Chemistry and Physics 2010;119:330.
[20] Boudjemaa A, Boumaza S, Trari M, Bouarab R, Bouguelia A. Physical and photo-electrochemical characterizations of α-Fe_2O_3. Application for hydrogen production. International Journal of Hydrogen Energy 2009;34:4268.
[21] Dan ZG, Ni HW, Xu BF, Xiong J, Xiong PY. Microstructure and antibacterial properties of AISI 420 stainless steel implanted by copper ions. Thin Solid Films 2005;492:93.
[22] Zhang ZX, Lin G, Xu Z. Effects of light pre-deformation on pitting corrosion resistance of copper-bearing ferrite antibacterial stainless steel. Journal of Materials Processing Technology 2008;205:419.

Please cite this article in press as: Atta NF, et al., Corrosion inhibition, hydrogen evolution and antibacterial properties of newly synthesized organic inhibitors on 316L stainless steel alloy in acid medium, International Journal of Hydrogen Energy (2011), doi:10.1016/j.ijhydene.2011.02.134